

SIMULATING FLOW ABOUT SCRAMJET COMBUSTION CHAMBER COMPONENTS IN WIND TUNNELS

V.I. Alfyorov and A.S. Bushmin

*Central Aerohydrodynamic Institute named after prof. N.E. Zhukovsky (TsAGI)
Zhukovsky, Russia*

Key words: scramjet; combustion chamber; heat flow, heat flux; wind tunnel with resistive heating; wind tunnel with MHD-acceleration of gas flow.

Abstract. Components of future aerospaceplanes include the scramjet which operates over the flight Mach number (M_{flight}) range from 5 to 20 while implementing supersonic burning of the fuel. When developing the combustion chamber for the scramjet, the following problems must be solved: mixing the fuel ingredients; establishing the supersonic combustion; and meeting the structure withstand temperature limitations. These problems are notably difficult to solve because flow within the combustion chamber is certainly three-dimensional, including the complicated pattern of interference of shock waves, flow separation areas, mixing of jet with various mass densities, and intense heat generation.

The article analyzes the problem of reproducing in wind tunnels the scramjet combustion chamber gasdynamic parameters: static pressure p_{st} , static temperature T_{st} , enthalpy H_0 , and Mach and Reynolds numbers. For a typical aerospaceplane flight path featuring the dynamic head $\rho v^2/2 = 0.75$ atm the stagnation parameters p_0 and T_0 are computed and compared with the parameters of TsAGI test facilities. IT is shown that at $M_{\text{flight}} \geq 8$ any of the existing test facilities fails to provide the conditions characteristic of the combustion chamber. Saying more specifically, a group of parameters – M and Re – may be reproduced in modernized hypersonic wind tunnels with resistive heating; and the other group – q , $T = T_w/T_0$, speed v , enthalpy H at the real-flight Mach number M – can be reproduced in wind tunnels with arc heaters and MHD-acceleration. The second group is essential when solving the third problem – developing the long-life structure because the areas of attaching the fuel struts to combustion chamber walls feature flow separation, complicated interference of shock waves and horse-shoe vortices, and heat flux concentration on both the struts and combustion chamber walls.

The article demonstrates the heat flux distribution over surfaces of a real fuel strut and a group of struts. Experiments were carried out in the TsAGI modernized hypersonic wind tunnel with resistive heating and in the wind tunnel with MHD-acceleration. Tests had covered the following ranges of parameters: $M_{\text{cc}} = 3, 4, 5,$ and 6 ; fuel strut blunting radius $R = 2, 3,$ and 4 mm; strut sweep angle $\Delta = 0, 10, 20, 30, 45,$ and 60 degrees. Heat fluxes were estimated by using temperature sensitive paints (TSP) and microcalorimeters. Theoretical analyses include solving the heat-conduction inverse problem by the regularization method. The pattern of shock waves was taken by using the shadowgraph; flow about the single strut and the strut group was visualized by using oil film. Heat flux values for the critical strut line are shown to be adequately described with the modified Fay–Riddell theory.

Scramjet operation is characterized with the wide range of variation of gasdynamic parameter fields within the combustion chamber – in what concerns flow speed, static pressure and temperature, Mach number, likely initial dissociation degrees, etc. For the M_∞ range from 8 to 20 the parameters would be as follows: $p_{\text{st}} = 8\text{--}0.5$ atm abs, $T_{\text{st}} = 800\text{--}2200$ K, combustion chamber Mach number $M_{\text{cc}} = 1.5\text{--}6.0$, and stagnation enthalpy of $2.0\text{--}20$ MJ/kg.

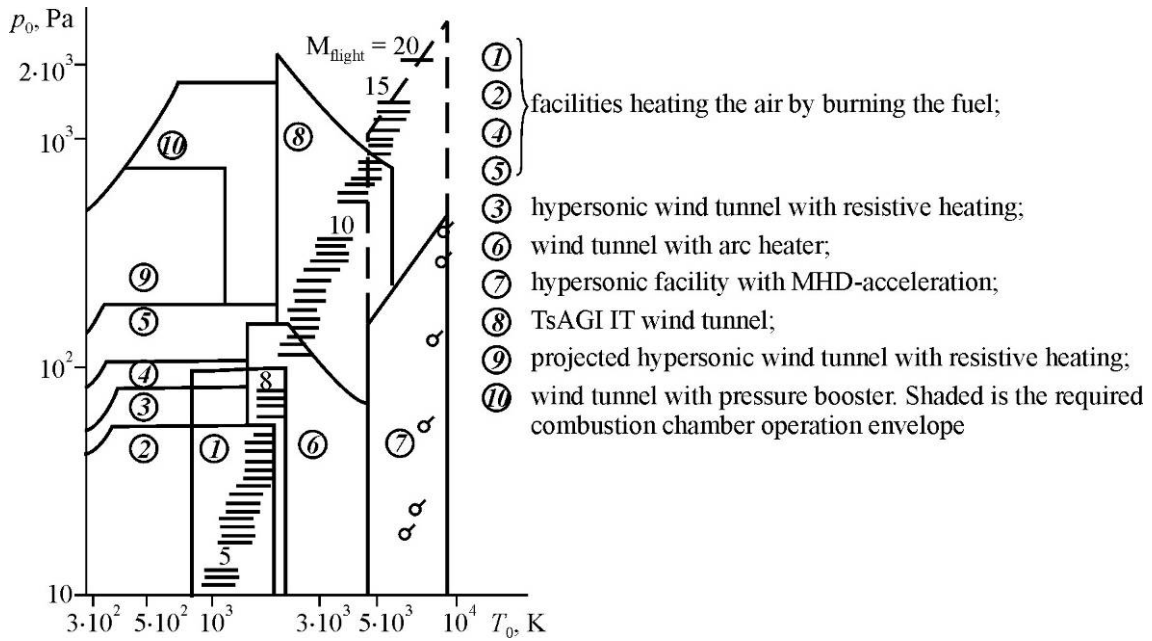


Figure 1. Operational envelopes of supersonic wind tunnels

Figure 1 shows the temperature–pressure envelope (for the wind tunnel stilling chamber) required for reproducing the static flow parameters prescribed. The numbers in circles designate the work ranges of the existing wind tunnels.

M_{cc} , Re , and Pr may be accurately ensured by the hypersonic wind tunnel with resistive heating. However, it cannot meet the requirement for the temperature factor T_w/T_0 . The necessary stagnation pressures and temperatures are reported in Table 1.

M_{flight}	5	8	10	12	15	20
M_{cc}	1.75	3.0	3.79	4.4	5.2	6.1
$Re_{cc} \cdot 10^{-5}$	Exact reproduction	1.32	0.92	0.8	0.58	0.32
$Re \cdot 10^{-5}$	Exact reproduction	3.2	1.8	1.16	0.64	0.42
p_0 , atm abs	14	1.7	5	10	10	30
T_0 , K	1200	300	400	600	650	900
p_{st} , atm abs	2.5	0.048	0.0485	0.039	0.015	0.017
T_{st} , K	800	105	105	105	100	100

Table 1

For providing the real-flight enthalpy and the respective heat flux of 50 MW/sq.m the most suitable facility is the hypersonic wind tunnel with MHD-acceleration. Flow parameters sufficient for simulating flow around the fuel strut downstream of the 90 by 120 mm nozzle are shown in Table 2 (p'_0 is the total pressure downstream of shock wave).

	p_{st} , atm abs	T_{st} , K	ρ , kg/m ³	v , m/s	M	p'_0 , atm abs	H_0 , kJ/kg
With MHD-acceleration	0.002	1100	$5 \cdot 10^{-4}$	4980	7.4	0.1	20
Without MHD-acceleration	0.0014	530	$9.3 \cdot 10^{-4}$	2521	5.7	0.054	5.8

Table 2

Given these parameters, the real (physical) speed, static temperature, chemical composition, and enthalpy are ensured; however, requirements for static pressure and Re_{cc} are not met.

To analyze flow around struts, the TsAGI T-120 hypersonic wind tunnel had been engaged; it offers ranges of temperature from 300 to 1100 K and of total pressure from 5 to 70 atm abs. Shaped nozzles have been manufactured to provide $M = 3, 4,$ and 5 ; the nozzle exit diameter is 150 mm. The Toepler device was used to photograph the strut flow pattern. Boundary layers on both the wall imitating the combustion chamber wall and the very strut were visualized by utilizing the graphite/oil film. The heat flux field over the strut was studied by using temperature sensitive paints. Areas of particular interest have been equipped with microcalorimeters.

To carry out studies at real-flight enthalpy values, the hypersonic wind tunnel with MHD-acceleration had been selected. It is described in [1]. The MHD channel includes 60 electrodes and a magnet with the field strength $B = 2.38$ T. The nozzle provides $M = 7$. Stagnation parameters are $T_0 = 8800\text{--}9800$ K and $p_0 = 45\text{--}110$ atm. The run duration is 0.5 s. The isentropic flow core size is 50 by 110 mm. The arc heater ($T_0 = 3800$ K) was employed alone and jointly with the MHD accelerator.

Fuel strut models were wing airfoils with the sweep angle $\Delta = 0, 10, 20, 30, 45,$ and 60 degrees, the fuel strut blunting radius $R = 2, 3,$ and 4 mm, the width of 80 mm, and the height of 80 mm. To make the same models suitable for tests in wind tunnels with the notable difference in heat fluxes, the models have been made of aluminum alloys and anodized to ensure the Al_2O_3 layer to be as thick as 0.3 mm; this hampers heat from spreading over the strut surface during a test run.

To measure heat flux over the upstream critical line of a strut, the calorimeter design was the copper plate 1 mm thick and 20 mm wide. The microcalorimeters inserted in the strut were copper cylinders with the 2 mm length and 2 mm diameter. Their thermal protection against heat flow from the strut was reliable. The calorimeter heating rate was measured by using chromel/copel thermocouples whose electrode diameter was 0.3 mm. Thermocouple signals were recorded by an oscillograph.

The calorimeter readings (i.e., temperatures) were used to evaluate the heat flux field on the basis of the inverse-problem solution method proposed by A.N. Tikhonov (see [2]). Heat flux over the leading-edge critical lines of struts was determined for the aforementioned sweep angles and blunting radii. Results are provided in Figure 2.

The strut leading-edge heat fluxes obtained in the T-120 facility at the various sweep angles suggest the heat flux does not depend on time and a calorimeter transverse coordinate. In

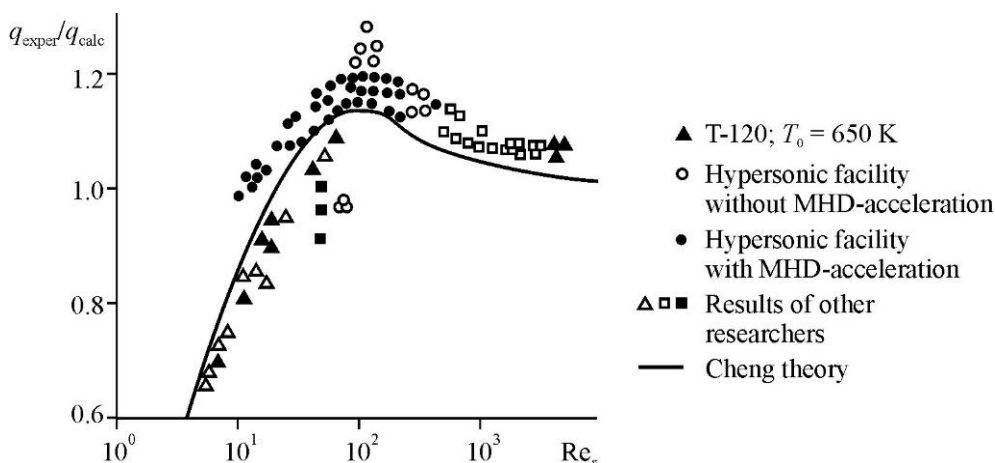


Figure 2. Experimental data vs. results of other researchers

the hypersonic wind tunnel with MHD-acceleration, Re number differs significantly, but the results turn out to be very similar.

The experimentally obtained heat fluxes were compared with values provided by the modified Fay–Riddell theory with the correlation function by Kohan for the flow spreading line on the leading edge of the cylinder installed at the yaw angle Δ , assuming the corresponding real gasdynamic parameters:

$$q = 0,57 \text{Pr}^{-0,6} (H_r - h_w) (\rho_s \mu_s)^m (\rho_w \mu_w)^{1/2-m} \sqrt{\beta_s};$$

$$H_r = H_0 - 0,075 (v_\infty \sin \Delta)^2; \quad \beta_s = \sqrt{2(p_s - p_\infty) / \rho_s},$$

where H_0 , H_r , and h_w are the total enthalpy, recovery enthalpy, and enthalpy at the wall temperature, respectively; p_s is the total pressure downstream of shock wave for the flow speed $v_\infty \cos \Delta$; r is the strut blunting radius; $m = 0.45$ for the cold wall (over the Re range from 10^4 to $4 \cdot 10^8$ the St number doesn't depend on p_0 in the wind tunnel stilling chamber).

Experimental and theoretical results are represented with the ratio $q_{\text{exper}}/q_{\text{calc}}$, Figure 2. As for the T-120 wind tunnel, the ratio doesn't depend on the strut sweep angle and blunting radius and on Re number, the ratio being 1.05–1.10. For the hypersonic wind tunnel with MHD-acceleration (as well as for tests with arc heating with no acceleration) the ratio is 0.9, also not depending on the above parameters.

Thus, the Fay–Riddell equation is suitable for determining heat fluxes over the covered ranges of Re, sweep angle, and stagnation enthalpy H_0 .

At lower gas density (when MHD-acceleration is implemented) the viscous flow is seen in a notable part of the shock layer. This phenomenon is properly described with the Cheng theory, refer to [3].

Figure 2 compares the theory with our test data (obtained in various facilities) and with data from other researchers. These are seen to converge rather well.

The struts with non-catalytic surfaces feature a lower heat flux as compared with data in [3]. These results were obtained in flow with turbulence intensity $\varepsilon = 1\text{--}2\%$. The presence of walls, the mutual influence of struts, and inhomogeneous and more intense turbulence may notably affect the results.

The work stage 2 engaged the T-120 wind tunnel to investigate flow about a single strut and a set of struts mounted at various distances between them. The struts feature the sweep angle $\Delta = 45^\circ$ and the blunting radius $r = 3$ mm. To vary thickness of the boundary layer upstream of struts, the wall imitating the combustion chamber wall had been complemented with special plates, of which one edge was attached to the nozzle exit section, and the opposite edge, to the diffuser entry section. Flow about the wall and the strut side surface was visualized with the oil/graphite film. The TSP was also utilized. Figure 3 demonstrates photographs of strut flow visualized. Flow about the single strut was studied and the flow patterns were acquired due to the oil film and the TSP to outline five characteristic zones over the strut: 1, tail zone; 2, mid-strut zone featuring the uniform flow; 3, trailing vortex zone; 4, zone where shock wave from the separation

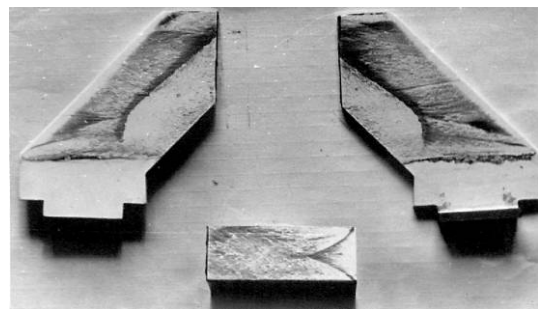


Figure 3. Flow photograph. $L = 40$ mm, $H = 35$ mm, $M = 3$, $d_c = 104$ mm, $p_0 = 3 \cdot 10^5$ Pa, $T_0 = 293$ K

area upstream of the strut interacts with the boundary layer; and 5, leading-edge critical line. Each of the zones features particular flow details and particular heat-transfer laws. These zones had been equipped with microcalorimeters.

Thereafter, flow about the set of struts was studied. The distance L between them was varied in steps: 20, 30, 40, 50, 60, and 70 mm. Mach number was established at 3, 4, and 5. At the distance of 20, 30, and 40 mm the shock wave interference pattern is certainly symmetric. At larger distances the separation zone notably shifts to the trailing edge. At $L = 50$ mm the flow pattern is similar to that for a single strut. The flow pattern on the wall imitating the combustion chamber wall also depends on the distance between struts. At $L = 20$ –30 mm there exists a pseudoshock with several separation zones. At $L = 40$ –50 mm one can see the horse-shoe vortex and a symmetric flow separation zone in between struts. At $L = 50$ –60 mm and larger values shock waves intersect in a regular manner. Flow downstream of the intersection line is supersonic. Seen downstream is a tangential speed discontinuity. At the distance of 40 mm the interference is such that there appears the Mach disk with a subsonic flow domain.

A computer generated image of shock wave interference near struts is provided in Figure 4.

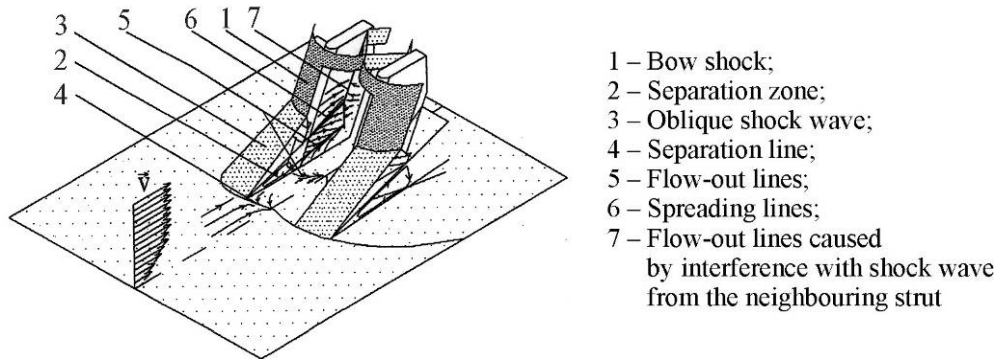


Figure 4. A schematic of flow around struts

The heat flux values based on microcalorimeter readings were compared with those produced by the Spalding–Chi theory for turbulent boundary layer and Reynolds numbers based on the distance from the leading edge, to show that in the zone 2 (as numbered above) the heat flux almost coincides with the theoretical values, so $q_{\text{exper}}/q_{\text{calc}} = 1$. For the zone 3, the ratio equals 2. The heat flux in the zone 1 depends on the strut-to-strut distance (note that shock waves do not hit the struts) and is 2.2 at $L = 40$ mm, 1.2 at $L = 60$ mm, and 1.1 at $L = \infty$.

The general picture of heat fluxes as determined by the TSP method is similar to those above, but particular values turned out to be slightly lower.

The zone 3 (related to the strut trailing edge) features a heat flux peak caused by boundary layer separation due to the vortex. The domains of increased heat fluxes coincide with separation zones revealed by the oil film.

These findings may be summarized as follows.

1. Flow parameters typical of the scramjet combustion chamber at $M > 8$ can be reproduced in facilities of various classes in the complex test. Required M_{cc} and Re_{cc} can be ensured in modernized hypersonic wind tunnels with resistive heating of gas in the stilling chamber. Heat fluxes, M_{cc} , real-flight enthalpy, and flow speeds can be ensured in facilities with MHD-acceleration; and combustion chamber structure heating can be ensured in facilities with arc heating.

2. Heat transfer to fuel struts and their models was analyzed in the hypersonic wind tunnel at real-flight Reynolds and Mach numbers for the combustion chamber, as well as in the hypersonic wind tunnel with MHD-acceleration at real-flight flow speeds, real-flight enthalpy, Mach number, and real-flight heat fluxes. It is shown that heat flux over the leading-edge critical line on a strut with the sweep angle of 0 through 60 degrees and the blunting radius of 2, 3, and 4 mm is described with the Fay–Riddell relation and Kohan correction, the error being $\pm 10\text{--}15\%$. To improve analyses, the Cheng theory should be involved, which allows for viscosity and entropy effects; in addition, flow non-equilibrium should be taken into account.

3. At real-flight numbers M_{cc} and Re_{cc} the flow pattern in the boundary layer and in between struts was clarified at various values of distance between them. Interference types have been established. The temperature sensitive paint and microcalorimeters were utilized to determine heat flux fields over struts; these are shown to be essentially inhomogeneous. Heat fluxes for various domains of struts have been evaluated. Some correlations are proposed.

REFERENCES

- [1] Alfyorov V.I., Vitkovskaya O.N., Shcherbakov G.I., Rukavets V.P., Rudakova A.P. Gas-dynamic wind tunnel with MHD gas acceleration. 10-th International Conference on MHD generators. India. Vol. I, p. VII.31 (1989).
- [2] Batura N.I. Degree of instability of numerical solution of inverse problems of heat conduction; error in test data. // IFZh, vol. 56, no. 3, pp. 446–450 (1989).
- [3] Cheng H.K. The Blunt Body Problem in Hypersonic Flow at Low Reynolds Numbers. //IAS paper no. 63-92 (1963).